

UC Berkeley

Postprints from CPL

Title

An enthalpy-temperature hybrid method for solving phase change problems and its application to polymer pyrolysis and ignition

Permalink

<https://escholarship.org/uc/item/5zb7w2p5>

Journal

COMBUSTION THEORY AND MODELLING, 4(4)

Authors

Zhou, Ying-Ying
Fernandez-Pello, Carlos

Publication Date

2000-12-01

Peer reviewed

**An enthalpy-temperature hybrid method for solving phase change
problems and its application to polymer pyrolysis and ignition**

Y. Zhou and A. C. Fernandez-Pello^{*}
Department of Mechanical Engineering
University of California at Berkeley
Berkeley, CA 94720-1740, USA

Phone: (510) 642-6554

Fax: (510) 642-1850

ferpello@newton.me.berkeley.edu

Short Title: Enthalpy-temperature method and its application

^{*} Corresponding author

An enthalpy-temperature hybrid method for solving phase change problems and its application to polymer pyrolysis and ignition

Y. Zhou and A. C. Fernandez-Pello
Department of Mechanical Engineering
University of California at Berkeley
Berkeley, CA 94720-1740, USA

Abstract

In this work, an enthalpy-temperature hybrid method is proposed for the numerical solution of generalized phase change problems, and applied to the prediction of polymer pyrolysis and ignition. The basic idea of this method is to treat both enthalpy and temperature as independent variables, and to solve the conservation equations and the constitutive equations (enthalpy-temperature relations) simultaneously. The formula of the enthalpy-temperature relations are not necessarily the same for different phases, but can be chosen independently according to the characteristics of physical problems and the convenience of numerical analysis for each respective phase. Therefore this method applies to the problems regardless of the form of the constitutive equations. It overcomes the difficulty or even impossibility encountered in the traditional enthalpy-temperature method, of which either enthalpy or temperature must be consistently and explicitly expressed as a function of the other over all the phases. The method is first applied to a one-dimensional classical freezing problem for method demonstration and verification. It is found that the numerical results of temperature history and the position of phase change interface agree well with the analytic solution existing in the literature. The method is then applied to the numerical simulation of the pyrolysis and ignition of a composite material with a polymer as the matrix and fiberglass as the filling material. Three models of oxygen distribution in the molten layer are considered to explore the melting and oxygen effects on the polymer pyrolysis. Numerical calculation shows that high oxygen concentrations in the molten layer enhance the pyrolysis reaction, resulting in a larger amount of pyrolysate, but in lower surface temperatures of the sample. It also shows that distribution of oxygen in the molten layer has a strong effect on pyrolysate rate, and therefore on ignition and combustion of polymers. Comparison with available experimental data indicates that a model of oxygen distribution in the molten layer that is limited to a thin layer near the surface describes best the ignition process for a homogeneously blended polypropylene/fiberglass composite.

1. Introduction

The combustion of polymers is a complex phenomenon that involves chemical and physical processes in both gas and condensed phases. Concerning specifically the ignition of solid polymeric fuels, under the condition of fast chemical kinetics, thermo-chemical processes in the condensed phase primarily determine their ignition characteristics. This is because the necessary condition for ignition is the attainment of a certain fuel concentration in the gas phase (related to the lean flammability limit), which in turn is dependent on the attainment of a specific pyrolysate generation rate. The thermo-chemical processes that are particularly important in the polymer pyrolysate generation are pyrolysis kinetics, phase change, and heat and mass transfer in a multi-phase medium. Pyrolysis has been studied extensively from the viewpoints of chemical kinetics and physical mechanisms [1-7]. It has also been investigated numerically[8-11]. Melting, and its effect on pyrolysis, however, has been given much less attention, although there is evidence that melting may play an important role in the combustion of polymers[12,13], and thus there is need for further understanding of the combined effect of pyrolysis and melting on the combustion of polymeric materials.

The melting temperature of thermoplastics is relatively low, and hence melting process in general precedes the ignition. The material's phase and physical properties undergo a change after melting, and motion might be induced in the molten layer, which would enhance the diffusion and mixing of oxygen within the polymer. For some thermoplastics, oxygen concentration has negligible effect on the pyrolysis of the condensed phase, so that melting of the material only serves as a heat sink by absorbing a certain amount of energy. The result is a comparatively low temperature, and as a

consequence of the Arrhenius law, a relatively low pyrolysis rate compared to that of pyrolysis without melting. For other thermoplastics, oxygen interacts with the polymers during the pyrolysis process, through what is known as oxidative pyrolysis. It is likely that oxidative pyrolysis contributes significantly, or even predominantly, to the liberation of volatile and combustible fragments from the polymers[3,5]. The rate of oxidative pyrolysis depends on the local oxygen concentration, and the composition of oxidative products may vary with different oxygen concentration. For this type of thermoplastics, melting has more profound effects on ignition and combustion of the material due to oxygen penetrating into the sample. For this reason, accurate prediction of phase change in the condensed phase is essential in the simulation of the combustion of thermoplastics.

Heat transfer with melting has been studied extensively because of its great importance in many industrial applications, such as casting, welding, thermal energy storage, crystal growth, and laser beam surface melting. Typically, numerical methods for solving phase change problems can be characterized into three categories: front-tracking methods, front-fixing methods and fixed-domain methods. Among them, the enthalpy method (one of the fixed-domain methods) appears to be favored by many investigators. The advantage of this method is that it applies to the whole domain regardless of the phase at a particular material point, which in turn implies that the tracking of the phase change interface is unnecessary. Moreover, the enthalpy method is applicable to problems in which phase change occurs either at a single temperature or over a temperature range. See [14, add 2 reference referee suggested here].

Most applications of the enthalpy method[15-20] treat only enthalpy as a control variable and express temperature (or Kirchoff temperature) as a function of enthalpy. The

enthalpy-temperature relation is incorporated into the formulation to eliminate the temperature from the governing equations. From a mathematical viewpoint, this treatment has merit over the method of directly using temperature as a control variable. For a phase change problem, temperature as a function of enthalpy is continuous over the whole range including the phase change point whereas enthalpy as a function of temperature exhibits a discontinuous point at the phase change temperature. However, as mentioned by Elliott and Ockendon[21], this treatment depends crucially on enthalpy being a monotonic increasing function of temperature. It applies only to certain idealized situations in which several thermal parameters are restricted. The simplest case is the one that all thermal parameters are constants. A majority of applications[15-18,22] assume that the specific heat is constant in order to get an explicit function of temperature related to enthalpy. Elliott and Ockendon[21] also point out that there is no obvious extension of this treatment to more generalized Stefan problems, such as a problem in which heat and mass transfer is coupled

In this work, a numerical treatment for the enthalpy-temperature method is proposed, which applies to any phase change problem regardless of the form of the material's constitutive equations. It treats both enthalpy and temperature as independent variables and solves the enthalpy-temperature relation simultaneously in conjunction with the energy conservation equation, or with all the governing equations if mass, momentum and species are involved. The formula of the enthalpy-temperature relations in different phases are not necessary the same (either enthalpy as a function of temperature or temperature as a function of enthalpy), but can be chosen independently according to the characteristics of physical problems and the convenience of numerical analysis for each

respective phase. For instance, temperature as a function of enthalpy can be specified for solid phase whereas enthalpy as a function of temperature can be used for liquid phase in which the relation otherwise would be impossible to obtain. The freedom of choosing the form of the constitutive equations in different phases overcomes the difficulty or even impossibility encountered in the traditional enthalpy-temperature method, of which either enthalpy or temperature must be consistently and explicitly expressed as a function of the other over all the phases. Historically, the idea of solving the enthalpy-temperature relation together with the energy equation was explored to some extent by Crowley[22], but a constant specific heat was assumed and temperature as an explicit function of enthalpy was adopted. Here, these limitations are eliminated and the method is applicable to general phase change problems.

To verify the predictive capabilities of the method proposed here, it is first applied to the numerical solution of a classical phase change problem[23] and compared with the existing analytical solution. The method is then applied to the prediction of the pyrolysis and ignition of a composite combustible material in which a thermoplastic (polypropylene) is the matrix and fiberglass the filling material. Representative numerical results are compared with available experimental data.

2. Enthalpy-temperature hybrid method

Consider a simple heat conduction problem in one dimension. Assuming the heat conduction follows the Fourier's law, the transient energy conservation equation can be expressed as:

$$\frac{\partial(\rho h)}{\partial t} = \frac{\partial}{\partial x} \left(k \frac{\partial T}{\partial x} \right) \quad (1)$$

For simplicity, here \mathbf{r} and k are assumed as constants. Thus in equation (1), there are two variables, temperature T and enthalpy h , to be determined. These two variables are related by the thermodynamic enthalpy-temperature relation, referred to hereafter as the constitutive equation, which can be highly nonlinear and can exhibit jumps. For the materials whose phase change occurs at a single temperature T_m , the enthalpy-temperature relation may be written as:

$$h = \int_0^T C_{ps} dT \quad h < h_{solid} = \int_0^{T_m} C_{ps} dT \quad (2a)$$

$$T = T_m \quad h_{solid} \leq h \leq h_{solid} + L \quad (2b)$$

$$h = h_{solid} + L + \int_{T_m}^T C_{pl} dT \quad h > h_{solid} + L \quad (2c)$$

Notice that the enthalpy-temperature relation is specified by integral equations in the solid and liquid phases whereas the phase change point is characterized by $T=T_m$ with the condition of $h_{solid} \leq h \leq h_{solid} + L$. **Formulation like equation (2) enables the proposed enthalpy method applicable to the problems whose constitutive equations cannot be expressed simply as a single function in terms of one independent variable (either enthalpy or temperature) over all the possible phases. For instance, a phase change occurs at a discrete melting temperature with temperature-dependent heat capacity so that temperature cannot be expressed as an explicit function of enthalpy in solid or/and liquid. In this case, enthalpy as a function of temperature can be used in solid or/and liquid, but not at the melting point because the value of enthalpy is undetermined at this point. So neither enthalpy nor temperature can be specified explicitly as a function of the other over all the possible phases. For this reason, the traditional enthalpy-temperature method**

fails unless other approximation (such as smoothing over a small temperature zone) is adopted.

As stated before, the basic idea of this method is to treat both enthalpy and temperature as independent variables. The numerical solution proceeds as follows. The energy equation is discretized using the standard finite difference method, resulting in a set of algebraic equations involving the nodal values of both T and h . Then, these equations are augmented with the constitutive equations at every node point. At each iteration, the phase of every node point is checked and the constitutive equations are selected accordingly. The major advantage of this method is that it applies regardless of the form of the constitutive equations; therefore the most appropriate equation can be selected for each respective phase. In addition, during phase change, the relation (2b) is enforced, hence the temperature is fixed at the correct value, and the enthalpy is determined by the balance of energy conservation.

In the actual implementation of the method, the expanded equations are not explicitly constructed for some problems with simple constitutive equations; instead, the constitutive equations at each node point can be linearized and essentially eliminated locally. In this case the number of the actual algebraic equations involved in Newton-Raphson iteration equals the number of nodes in the system, and the computation time is roughly the same as that of solving only the discretized energy conservation equation. For other problems with complicated constitutive equations, T and h have to be solved simultaneously.

3. Verification of the method

The classical Stefan problem is one of the few phase change problems that have analytic solutions. Thus it is good to be used as a benchmark to verify the method proposed above. It is a one-dimensional freezing problem of a semi-infinite slab initially in liquid phase with a uniform constant temperature. At time $t = 0$, the temperature on the surface $x = 0$ is suddenly dropped to a value below the material melting temperature and maintained at this value as time goes on. This initiates solidification within the slab. As time increases, the interface of phase change propagates through the slab. The governing equation and the enthalpy-temperature relation are the same as equation (1) and (2). The initial and boundary conditions for this problem are summarized as follows:

$$\begin{aligned} h|_{t=0} &= h(T(x,0)) \\ T|_{x=0} &= T(0,t) \quad T|_{x=\infty} = T(\infty,t) \end{aligned} \quad (3)$$

Rubenstein[23] has derived an analytical solution for this freezing problem. The position of phase change interface and the temperature history at any position as functions of time are,

$$X(t) = 2I(\mathbf{a}_s t)^{1/2} \quad (4)$$

and

$$T = \begin{cases} T(0,t) + \frac{T_m - T(0,t)}{\text{erf}I} \text{erf}\left(\frac{x}{2(\mathbf{a}_s t)^{1/2}}\right) & x < X(t) \\ T_m & x = X(t) \\ T(x,0) + \frac{T_m - T(x,0)}{\text{erfc}(I(\mathbf{a}_s / \mathbf{a}_l)^{1/2})} \text{erfc}\left(\frac{x}{2(\mathbf{a}_l t)^{1/2}}\right) & x > X(t) \end{cases} \quad (5)$$

where I is a constant evaluated from the following equation,

$$\frac{e^{-I^2}}{\text{erf}I} - \frac{k_l}{k_s} \frac{\mathbf{a}_s^{1/2} (T(x,0) - T_m) e^{-\mathbf{a}_s I^2 / \mathbf{a}_l}}{\mathbf{a}_l^{1/2} (T_m - T(0,t)) \text{erfc}(I(\mathbf{a}_s / \mathbf{a}_l)^{1/2})} = \frac{ILp^{1/2}}{C_s(T_m - T(0,t))} \quad (6)$$

For the numerical solution of this problem with the method proposed here, the finite difference grids with uniform spacing are used (see Fig. 1). The control volume method[24] is used to discretize the governing equation (1). The ensuing equation, together with equations (2) and (3), results in a set of algebraic equations, which are solved numerically by the full Newton-Raphson iteration method[25] to obtain temperature and enthalpy distributions along x at each time step.

A technique to numerically predicate the location of the phase-change interface similar to the idea of partially frozen elements in [18] is implemented. With known enthalpy distribution at each time step, the position of the phase change interface can be computed as the following (for this particular problem with this particular grids' arrangement),

$$X = \begin{cases} (i-1) \times dx & h_i \geq h_{solid} + L \\ (i - \frac{h_i - h_{solid}}{L}) \times dx & h_{solid} \leq h_i < h_{solid} + L \end{cases} \quad (7)$$

where i indicates the grid nearest to the front surface with enthalpy greater than h_{solid} , and dx the grid spacing. Equation (7) assumes that the solid and liquid phases are separated by a sharp moving interface (see Fig. 1.), and they co-exist in a grid of which the enthalpy is in the range of $[h_{solid}, h_{solid} + L]$. With the help of energy conservation, the portion of solid in the grid can be calculated, which leads to the prediction of the position of the solid-liquid interface.

To compare the analytical and numerical solutions, the data in Voller[18], listed below, are used. I is found to be equal to 0.2037 for this particular setting[14].

$$\begin{array}{lll}
 T_m = 0 & T(\infty, t) = 2 & T(x, 0) = 0 \\
 T(0, t) = -4 & k_s = k_l = 2 & \\
 C_s = C_l = 2.5 \cdot 10^6 & r_l = r_s = 1 & L = 100 \cdot 10^6
 \end{array}$$

The numerical and analytic results for the classical freezing problem are compared in Fig. 2 and 3. Figure 2 plots the position of the phase change interface as a function of time, and Fig. 3 plots the temperature histories at several positions in the slab. From Fig. 2 and 3, it is seen that the numerical and analytic results match very well with each other, which verifies that the proposed method is capable to solve phase change problems.

4. Application to the prediction of the pyrolysis and ignition of a composite

The problem considered in this analysis is illustrated in Fig. 4. The problem describes the experimental conditions of the Forced-flow Ignition and flame-Spread Test (FIST) developed at the micro-gravity combustion laboratory at UC Berkeley. FIST measures the piloted ignition delay and the rate of flame spread under various external heat fluxes, flow velocities and oxidizer concentrations. A detailed description of the FIST is given in [26]. The front surface of a sheet of a blended polypropylene/fiberglass (PP/GL) composite is suddenly exposed to a uniform, and constant, external radiant heat flux, and to a flow of oxidizer parallel to the solid surface. Its back surface is insulated to both heat and mass transfer. At first, the transient heating of the material is an essentially inert process, controlled by the balance of solid phase heat conduction, in-depth absorption of radiation, endothermic pyrolysis, and convective and radiant heat losses

from the exposed surface to the environment. The pyrolysis process is dominated by thermal pyrolysis, and its reaction rate is low due to **the large activation energy** and low temperature. Eventually, endothermic melting begins within the solid, and **the** melting front propagates through the matrix (PP). Once melting occurs, oxygen is diffused from the oxidizer into the molten layer, where it interacts with PP, and oxidative pyrolysis takes place with a rate depending on the local oxygen concentration. Thermal pyrolysis is still present in the rest of the solid. The evolved pyrolysate gas is diffused away from the surface mixing with the oxidizer flow. If the conditions are such that a flammable mixture is formed near the pilot, ignition occurs.

The objective of the present analysis is to capture the essential characteristics of the pyrolysis and ignition, while reducing the complexity of the mathematical problem; for this reason, the following assumptions are made in formulating the model:

- Since the external heat flux is uniform along the surface, and the sample characteristic length is much larger than its thickness, the problem is formulated one-dimensional.
- Thermal conductivity of the composite follows the mixture rules and depends locally on the transient density and temperature.
- Fiberglass (GL) in this composite is assumed to be uniformly distributed and inert.
- Motion within the molten layer is not considered.
- A first-order Arrhenius law is used to model the oxidative and thermal pyrolysis of polypropylene (PP). The chemical kinetic parameters for both pyrolysis rates are obtained from the experimental data of Stuetz *et al.*[7], and are functions of local oxygen concentration.

- Thermal equilibrium between polypropylene, fiberglass and trapped pyrolysate are assumed locally at every point of the medium.
- The pyrolysate flows through the multi-phase medium with no resistance.

With these assumptions, the resulting one-dimensional transient problem is represented by the following form of the mass and energy equations,

$$\frac{\partial \rho_{pp}}{\partial t} - \frac{\partial \dot{m}_{pv}}{\partial x} = 0 \quad (8)$$

$$\frac{\partial (\rho_{pp} h_{pp})}{\partial t} + \frac{\partial (\rho_{gl} h_{gl})}{\partial t} - \frac{\partial (\dot{m}_{pv} h_{pv})}{\partial x} = \frac{\partial}{\partial x} \left(k \frac{\partial T}{\partial x} \right) + Q_{pp} \frac{\partial \rho_{pp}}{\partial t} + \dot{q}_{rad, in-depth}'' \quad (9)$$

where

$$\mathbf{r}_{pp} = \mathbf{c}_{pp} \mathbf{r}_{pp,o}$$

$$\mathbf{r}_{gl} = (1 - \mathbf{c}_{pp,o}) \mathbf{r}_{gl,o}$$

$$h_{gl} = \int_0^T C_{gl,s} dT$$

$$h_{pv} = \int_0^T C_{pv,g} dT$$

$$\dot{q}_{rad, in-depth}'' = \epsilon \dot{q}_{rad}'' \left[\mathbf{c}_{pp,o} \mathbf{g}_{pp} \mathbf{a}_{pp} \exp\left(-\int_0^x \mathbf{a}_{pp} dx\right) + (1 - \mathbf{c}_{pp,o}) \mathbf{g}_{gl} \mathbf{a}_{gl} \exp\left(-\int_0^x \mathbf{a}_{gl} dx\right) \right]$$

The negative signs in the RHS of Eq. (1) and (2) are due to the assumed direction of mass flow rate, which is along the negative-x direction.

The Arrhenius law and a mixture rule for the composite thermal conductivity specified in this particular case are:

$$\frac{\partial \rho_{pp}}{\partial t} = -Z \rho_{pp} \exp\left(-\frac{E_a}{RT}\right) \quad (10)$$

$$k = \rho_{pp} k_{pp,o}(T) + (1 - \rho_{pp,o}) k_{gl,o}(T) + (\rho_{pp,o} - \rho_{pp}) k_{pv,o}(T) \quad (11)$$

The thermodynamic relation of enthalpy and temperature for PP is given as

$$\begin{aligned}
h_{pp} &= \int_0^T C_{pp,s} dT & h_{pp} < h_{pp,s} &= \int_0^{T_{pp,m}} C_{pp,s} dT \\
T &= T_{pp,m} & h_{pp,s} &\leq h_{pp} \leq h_{pp,s} + L_{pp} \\
h_{pp} &= h_{pp,s} + L_{pp} + \int_{T_{pp,m}}^T C_{pp,l} dT & h_{pp} &> h_{pp,s} + L_{pp}
\end{aligned} \tag{12}$$

The initial and boundary conditions are taken as:

at $t = 0$

$$\mathbf{r}_{pp,o} = \mathbf{c}_{pp,o} \mathbf{r}_{pp,pure} \quad \mathbf{r}_{gl,o} = (1 - \mathbf{c}_{pp,o}) \mathbf{r}_{gl,pure} = \mathbf{r}_{gl}$$

$$h_{pp,o} = h_{pp}(T_o) \quad h_{gl,o} = h_{gl}(T_o)$$

at $x = 0$

$$\mathbf{e}\dot{q}_{rad}'' [\mathbf{c}_{pp,o}(1 - \mathbf{g}_{pp}) + (1 - \mathbf{c}_{pp,o})(1 - \mathbf{g}_{gl})] = -k \frac{\mathcal{I}T}{\mathcal{I}x} + h_{conv} (T_{surf} - T_{amb}) + \mathbf{e}\mathbf{o}T_{surf}^4$$

at $x = L$

$$\frac{\mathcal{I}\dot{m}_{pv}}{\mathcal{I}x} = 0 \quad \frac{\mathcal{I}T}{\mathcal{I}x} = 0$$

For clarification purposes it is worth mentioning the following issues inherent in the above equations. First, in the energy equation (Eq. 9), enthalpy changes of PP and GL are considered separately, because GL remains in solid state and does not interact with PP during the pyrolysis process. This approach considerably simplifies the numerical computations.

Secondly, melting of PP is incorporated in the thermodynamic relation of enthalpy and temperature (Eq.12), and is assumed to occur at a fixed temperature. The value of this temperature is determined by fitting the numerical calculation to the experimental surface temperature measurement obtained in the FIST apparatus. As it is

shown below, the resulting melting temperature is smaller than the value in [27], which is defined as the equilibrium melting temperature for a pure, infinitely large PP crystal. However, the melting behavior of polymers, and in particular PP, is far more complicated than the process implicit in that definition, and depends on a number of factors, most notably crystallinity, molecular weight, molecular distribution, thermal history, rate of heating. In addition, GL in the composite may damage the crystallinity and function as the impurity, which results in a large depression of the melting temperature. Moreover, softening, recrystallization and annealing may also occur. Therefore, the use of an equilibrium temperature to identify melting of a PP/GL composite is a simplification of a much more complicated process, and it is justifiable to rely on comparison with experimental data to determine this pseudo-melting temperature, until more accurate determination of the melting process is conducted.

Thirdly, both oxidative and thermal pyrolysis processes are expressed by equation (10). Whether it represents oxidative or thermal pyrolysis depends on the pre-exponential constant and the activation energy, which are functions of the local oxygen concentration. In accordance with the experimental data in [7], see Fig. 5, the pre-exponential constant and the activation energy as functions of oxygen concentration can be approximated as,

$$\ln(-\ln Z/Z_0) = -0.14925 \times (\ln C)^2 + 0.45748 \times \ln C + 3.06028 \quad (13)$$

and

$$\ln(E_a/E_{a0}) = 0.01016 \times (\ln C)^2 - 0.15087 \times \ln C - 0.65272 \quad (14)$$

Here, Z_0 and E_{a0} are the experimental pre-exponential constant and the activation energy at zero oxygen concentration, the values of which are $Z_0 = 5.69484 \times 10^{16} \text{ s}^{-1}$ and

$E_{a0} = 58$ kcal/mol, respectively. Hence, if the local oxygen concentration is known, then Z and E_a can be obtained from (13) and (14). Substituting them into equation (10) leads to the corresponding pyrolysis.

4.1. Models for oxygen distribution in the molten layer

PP oxidation under most experimental conditions are considered as diffusion-limited[3,4,7]. Boss *et al.*[3] has reported a depth less than 0.6 mm from the sample surface as the oxidation region of PP, while Stuetz *et al.*[7] has shown a distribution of oxygen concentration below the burning surface of a rod after quenching with N₂. Stuetz *et al.*[7] has also observed a greater depth of oxidation region below the real burning surface, which they argued might be due to the motion of the molten layer. To describe these experimental observations and explore the melting and oxygen effects on pyrolysis and ignition, three models are considered for the oxygen distribution in the molten layer.

The first model assumes that the molten layer, when formed, is well stirred either by surface shear stress, by temperature gradient or by bubbling of released volatile. Considering the fact that diffusion in the solid is generally much slower than that in the corresponding liquid, the oxygen concentration in the liquid phase is taken as the same as that in the ambient whereas the oxygen concentration in solid phase remains zero. In another word, the oxidative pyrolysis takes place over the whole molten layer at the ambient oxygen concentration. At the beginning, the sample is in the solid phase and hence only thermal pyrolysis takes place. As time goes on, melting occurs and the melting front penetrates into the sample, the region of oxidative pyrolysis enlargers until

the melting front reaches the back face of the sample. At this moment, oxidative pyrolysis takes place over the whole sample.

The second model assumes that oxidative pyrolysis of PP is limited in a narrow region, a depth less than 0.6 mm from the sample surface, according to the observations by Ross[3]. In this model, oxygen concentration in a thin molten layer near the surface is assumed to be equal to that in the ambient. So the region of oxidative pyrolysis increases at first, and then remains constant (0.6 mm) after the melting front passes the critical line. Thermal pyrolysis takes place over the part of the sample with the depth greater than 0.6 mm whether it is melted or not.

The third model considers oxygen diffusion in the molten layer, and assumes no oxygen accumulated in the sample during pyrolysis. That is, oxygen diffused into the sample is balanced by the consumption of oxidative reactions, establishing a concentration gradient of finite depth beneath the surface. Assuming diffusion follows the Fick's law with a constant diffusivity D and reaction has a constant reaction rate of r , the conservation of oxygen concentration in the sample can be written as:

$$D \frac{d^2 C}{dx^2} - rC = 0 \quad (15)$$

Assuming that oxygen diffuses into the sample slower than the penetration of the melting front, then the boundary conditions for oxygen concentration are:

$$\begin{aligned} C &= C_0 & x &= 0 \\ C &= 0 & x &= l \text{ (position of the melting front)} \end{aligned} \quad (16)$$

Solving equation (15) and (16) leads to

$$C(x) = \frac{C_0}{e^{\sqrt{r/D}l} - e^{-\sqrt{r/D}l}} \left(e^{\sqrt{r/D}(l-x)} - e^{-\sqrt{r/D}(l-x)} \right) \quad (17)$$

Matching the above analytic solution to the experiment measurement in [7], we have

$$\sqrt{r/D} = 7.5 \text{ mm}^{-1}$$

Eq. (17) shows that the oxygen concentration is a steep function of position. That is, the oxygen concentration drops quickly in a very narrow region. It also shows that the oxygen concentration depends on the position of the melting front. As equation (13)~(14) and Fig. 5 indicate, the pre-exponential constant and the activation energy are highly sensitive to the oxygen concentration in the condensed phase, particularly when the local oxygen concentration is small. Therefore it is reasonable to expect that the melting process of the PP would play a role in the pyrolysis and ignition of the composite.

4.2. Numerical Results

The numerical analysis is applied to the description of the heating and pyrolysis of a PP/GL composite, commercially available from Montell North America Inc., as BJ22GC. This composite is one of the materials tested in the FIST apparatus. The composition and the geometric dimension of the sample used in the tests are as follows. The sheet contains 70% of PP and 30% of GL in volume, and is 1/8 inch (3.175mm) thick. Its properties are summarized in Table 1. The numerical calculations are compared to the experimental data for this standard PP/GL sample.

Figure 6 plots the numerical results of the pyrolysate mass flow rate vs. time at the external heat flux of 20 kw/m² and a given air flow velocity of 1.75 m/s, for the three oxygen concentration models. It shows that the pyrolysate mass flow rate varies noticeably with the different models described above. At the experimental ignition time, the pyrolysate mass flow rate from the first model is almost an order of magnitude higher

than the one from the third. Since the ignition is directly dependent on the fuel concentration in the gas phase, this implies that oxygen penetrating into the sample has a significant effect on the material's ignition and combustion. Thus accurately modeling oxygen concentration in the condensed phase, and hence the pyrolysate mass flow rate, is a prerequisite to simulate the ignition and combustion of polymers in gas phase.

To select which one of the above models best describes the present ignition process, we will rely here on available experimental data on pyrolysis rates for polypropylene under conditions similar to those studied here. It has been reported that the measured critical mass loss rate for the ignition of granular polypropylene is $2.2 \text{ g/m}^2\text{s}$ under natural convection and $2.7 \text{ g/m}^2\text{s}$ under forced flow convection [30-32]. Also, the mass loss rate at ignition for polypropylene can be estimated to be approximately $1 \text{ g/m}^2\text{s}$ from the measured ignition delay time and mass loss rates obtained using the cone calorimeter [29]. Although the critical mass loss rate for the ignition of fuel vapor-air mixture may be dependent on the experimental conditions, for the present case it should be more or less of the same order as that of the above measurements since the experimental conditions are similar. Thus, based on the results of Fig. 6 and the above data, the second model is selected as the one that describes best the pyrolysis rate.

Figure 7 plots the numerical results of the surface temperature history at the same conditions as in Fig. 6. It also plots the experimental result obtained with the FIST apparatus. The ripples in the experimental temperature profile are caused by the on and off switch that controls the heater output[26]. The results of Fig. 7 show that the surface temperatures for the three different models are distinguishable only after they reach to about $210 \text{ }^\circ\text{C}$. This means that it is at this point that significant pyrolysis occurs, and that

the energy used to decompose the polymer starts to play a role in the overall energy balance. Since the oxidative pyrolysis can be viewed as an oxygen-enhanced decomposition, the larger region of oxidative pyrolysis and the higher oxygen concentration lead to the faster chemical reaction and hence the larger amount of pyrolysate released as indicated in Fig 6. This, however, consumes more energy because its overall reaction is endothermic. That is why the difference in temperature is not as significant as that in pyrolysate mass flow rate and why the surface temperature of the first model is the lowest in Fig. 7. Nonetheless, comparison of the numerical and experimental results for the surface temperature also indicates, as with the pyrolysate mass flow rate, that the second model is the one that describes best the present problem.

That the second model predicts best the experiment data **can** be explained as follows. The forced gas flowing parallel to the surface, buoyancy in gas phase and in the molten layer, and bubbling can induce motion in the molten layer of the sample, and in turn enhance the mixing of oxygen with the material. However, the liquid polymer in the molten layer **is** quite viscous which, together with the homogeneously distributed fiberglass in the composite, **constrains** the motion of the molten material. Thus, except in a very thin layer close to the surface, the rest of the molten layer **is** quiescent, and consequently oxygen can only penetrate into the rest of the sample through molecular diffusion. Since the distribution of oxygen by diffusion **is** a very steep function of the distance from the surface, it is reasonable to infer that the oxygen concentration in the sample **is** small except near the surface. Therefore, in a very thin layer (<0.6 mm) near the sample surface pyrolysis **is** dominated by oxidative pyrolysis at approximately the

ambient oxygen concentration whereas in the rest of the sample it is dominated by the thermal pyrolysis, which is the assumption of the second model.

Ignition delay is one of the major factors that rank the materials' flammability. The implication is that under given oxidizer flow conditions, and heating rate, the ignition of the material is controlled by the attainment of a minimum concentration of fuel in the gaseous mixture adjacent to the pilot. This fuel concentration is logically related to the lean flammability limit. This criterion is used here, together with the second model of oxygen concentration in the molten layer, to predict the ignition delay over a wide range of external heat fluxes. The numerical results are shown in Fig. 8. The critical pyrolysate flow rates used here are determined by matching the numerical calculation with the experimentally measured ignition delay time at external heat fluxes of 20 kW/m^2 for 1 m/s and of 27.5 kW/m^2 for 1.75 m/s . They are $\dot{m} = 1.70 \text{ g/m}^2\text{s}$ (for air flow velocity of 1 m/s) and $\dot{m} = 1.78 \text{ g/m}^2\text{s}$ (for air flow velocity of 1.75 m/s) respectively. The FIST experimental results are also shown in Fig. 8. It is seen that the model predicts well the experimental result. The good agreement between them demonstrates the capability of this numerical model on simulating the pyrolysis and ignition of a composite material.

5. Conclusion

An enthalpy-temperature hybrid method has been developed to solve the generalized Stefan problem. The basic idea of this method is to treat all variables as independent variables, and to couple the constitutive equations, regardless of their forms, with the governing equations. Comparison with the analytic solution of the classical Stefan problem has confirmed its accuracy, and the application of this method in a model

of the pyrolysis and ignition of the PP/GL composite has indicated its capability in solving the complicated phase change problems.

Numerical results of the pyrolysis and ignition of the composite has shown that oxygen penetrating into the molten layer affects the pyrolysate mass flow rate and the surface temperature of the sample. High oxygen concentration enhances the pyrolysis, resulting in a larger amount of pyrolysate but in lower surface temperatures. Comparison with the experiments indicates that for a homogeneously blended PP/GL composite at least up to the ignition point, oxidative pyrolysis is limited to a thin layer near the sample surface (<0.6 mm). Since the pyrolysate rate is exclusively the fuel supply for gas phase combustion of solid combustible materials, accurately predicting melting and oxygen distribution within the condensed phase becomes a prerequisite for predicting the ignition and combustion of polymers.

Acknowledgments

This work was supported by National Aeronautics and Space Administration under Grant no. NCC3-478. The authors thank Mr. Mark Roslon, John Beck and Andreja Stevanovic for supplying the experimental data, and Dr. David C. Walther for his helpful comments.

Nomenclature

C	Specific heat, or oxygen concentration
D	Diffusivity of oxygen in polypropylene
E_a	Activation energy
h	Enthalpy
h_{conv}	Convection coefficient
k	Conductivity
L	Sample thickness
l	Position of melting front
L_{pp}	Latent of matrix in a composite
\dot{m}	Pyrolysate mass flow rate
\dot{q}_{rad}''	External radiant heat flux
$\dot{q}_{rad, in-depth}''$	In-depth radiant absorption
Q_{pp}	Heat of pyrolysis
R	Ideal gas constant
r	Reaction rate of oxidative pyrolysis
t	Time
T	Temperature
x	Coordinate along the sample thickness
Z	Pre-exponential factor in the Arrhenius law

GREEK

α	Radiant absorption coefficient
c	Effective volume fraction of matrix in a composite
ϵ	Emissivity of the sample
g	Fraction of in-depth absorption
ρ	Density

SUBSCRIPTS

<i>pp</i>	Matrix in a composite (Polypropylene)
<i>gl</i>	Fiberglass in a composite
<i>pv</i>	Pyrolysate
<i>o</i>	Initial
<i>pure</i>	pure materials
<i>s</i>	Solid
<i>l</i>	Liquid
<i>g</i>	Gas
<i>m</i>	Phase change
<i>surf</i>	Surface of the testing sample
<i>amb</i>	Ambient

Reference:

- [1]. Achimsky, L., Audouin, L. and Verdu, J., *Polymer Degradation and Stability* 57:231-240 (1997)
- [2]. Aseeva, R.M. and Zaikov, G.E., *Combustion of Polymer Materials*, Hanser Publishers, Munich Vienna New York, 1985
- [3]. Boss, C.R. and Chien, J.C.W., *J. Polymer Sci.: Part A-1*, 4:1543-1551 (1966)
- [4]. Brauman, S.K., *J. Polymer Sci.: Part B: Polymer Physics*, 26:1159-1171 (1988)
- [5]. Chien, J.C.W. and Kiang, J.K.H, *Stabilization and Degradation of Polymers*, Allara, D.L. and Hawkins, W.L. (eds), 1978, pp175-197
- [6]. Cullis, C.F. and Hirschler, M.M., *The Combustion of Organic Polymer*, Clarendon Press, Oxford, 1981
- [7]. Stuetz, D.E., Diedwardo, A.H., Zitomer, F. and Barnes, B.P. *J. Polymer Sci.: Polymer Chemistry Edition* 13:585-621 (1975)
- [8]. Nelson, M.I., Brindley J. and McIntosh, A., *Math. Comp. Modelling* 24:39-46 (1996)
- [9]. Staggs, J.E.J., *Fire Safety Journal* 32:17-34; 221-240 (1999)
- [10]. Sohn, Youngmin, Beak, S. W. and Kashiwagi, T., *Combust. Sci. Tech.*, 145:83-108 (1999)
- [11]. Butler, K.M., "A Mixed Layer Pyrolysis Model for Polypropylene", to appear in the Proceedings for the Sixth International Symposium on Fire Safety Science, Poitiers, France, July 5-9, 1999
- [12]. Kashiwagi, T., Omori A., and Nanbu H., *Combustion and Flame* 81:188-201 (1990)

- [13]. Kashiwagi, T., *25th Symposium (Int.) on Combustion*, The Combustion Institute, Pittsburgh, PA, 1994, pp.1423-1437
- [14]. Crank J., *Free and Moving Boundary problems*, Clarendon Press, Oxford, 1984
- [15]. Cao Y. and Faghri A., *Int. J. Heat and Mass Transfer*, 32:1289-1298 (1989)
- [16]. Crowley A. B. and Ockendon J. R., *Int. J. Heat and Mass Transfer*, 22:941-947 (1979)
- [17]. Hunter L. W. and Kuttler J. R., *J. Heat Transfer*, 111:239-242 (1989)
- [18]. Voller V. and Cross M., *Int. J. Heat and Mass Transfer*, 24:545-556 (1981)
- [19]. Hu H. and Argyropoulos S. A., *Modeling Simul. Mater. Sci. Eng.*, 3:53-64 (1995)
- [20]. Voller V. R., Cross M. and Markatos N. C., *Int. J. for Num. Methods in Eng.*, 24:271-284 (1987)
- [21]. Elliott, C. M. and Ockendon J. R., *Weak and Variational Methods for Moving Boundary Problems*, Pitman, London, 1982
- [22]. Crowley A. B., *Int. J. Heat and Mass Transfer*, 21:215-219 (1978)
- [23]. Rubenstein, L., *The Stefan Problem*, Transactions in Mathematics Monograph No. 27. American Mathematical Society, 1971
- [24]. Patankar, S.V., *Numerical heat transfer and fluid flow*, McGraw-Hill, 1980
- [25]. Isaacson, E. and Keller, H.B., *Analysis of Numerical Methods*, Dover, 1994
- [26]. Cordova, J.L., Zhou, Y., Pfaff, C.C. and Fernandez-Pello, A.C., in *Prevention of Hazardous Fires and Explosions*, Zarko, V.E. et al. (eds) 1999, pp.49-59
- [27]. Quirk R.P. and Alsamarraie M.A.A., *Polymer Handbook*, 1989, pp v/27-v/29
- [28]. Lubin, G. (ed), *Handbook of Composites*, 1981, p140
- [29]. Hopkins, D. Jr and Quintiere, J.G., *Fire Safety Journal*, 26:241-268 (1996)

- [30]. Drysdale, D., *An introduction to fire dynamics*, John Wiley and Sons, 1985, p217
- [31]. Tewarson, A., Lee, J.L. and Pion, R.F., *18th Symposium (Int.) on Combustion*, The Combustion Institute, Pittsburgh, PA, 1981, pp.563-570
- [32]. Tewarson, A. in *Flame-retardant Polymeric Materials*, Lewin, M. *et al.* (eds), 3:97-153 (1982)

Table 1. Physical properties of PP and GL

r_{pp}^a	kg/m ³	900	k_{pp}^a	W/mK	0.24
$C_{pp,s}^a$	J/kgK	10.1T - 1230	$C_{pp,l}^a$	J/kgK	5.2T + 932.8
L_{pp}^a	J/kg	2.09x10 ⁵	r_{gl}^b	kg/m ³	2500
k_{gl}^b	W/mK	0.33	$C_{gl,s}^b$	J/kgK	825
Z^c	1/s	2.3x10 ⁶ (oxidative) 4.6x10 ¹⁰ (thermal)	E_a^c	J/mol	8.79x10 ⁴ (oxidative) 2.43x10 ⁵ (thermal)
Q_{pp}^d	J/kg	1x10 ⁶ (oxidative) 3x10 ⁶ (thermal)	$T_{pp,m}^e$	K	360

^a Quirk *et al.*[27]

^b Lubin[28]

^c Stuetz *et al.*[7]

^d Hopkins[29]

^e Obtained from fitting numerical results to the experimental data in FIST

Captions

Figure 1. Discretization of the classical Stefan problem

Figure 2. Position of the phase change interface vs. time for the classical Stefan problem

Figure 3. Comparison of numerical and analytic temperature history at several positions for the classical Stefan problem

Figure 4. Schematic of the pyrolysis and ignition of a composite

Figure 5. Pre-exponential constant and activation energy as a function of oxygen concentration

Figure 6. Predicted oxygen concentration effect on the pyrolysis mass flow rate for the three models of oxygen distribution

Figure 7. Predicted variation with time of the sample surface temperature for the three models

Figure 8. Predicted external heat flux effect on ignition delay for two flow velocities using the second model

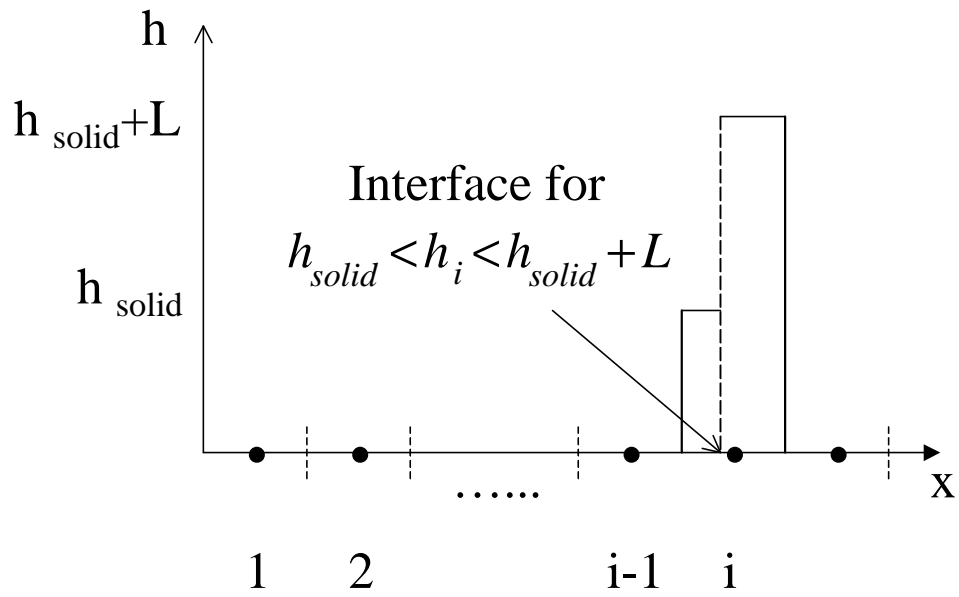


Figure 1. Discretization of the classical Stefan problem

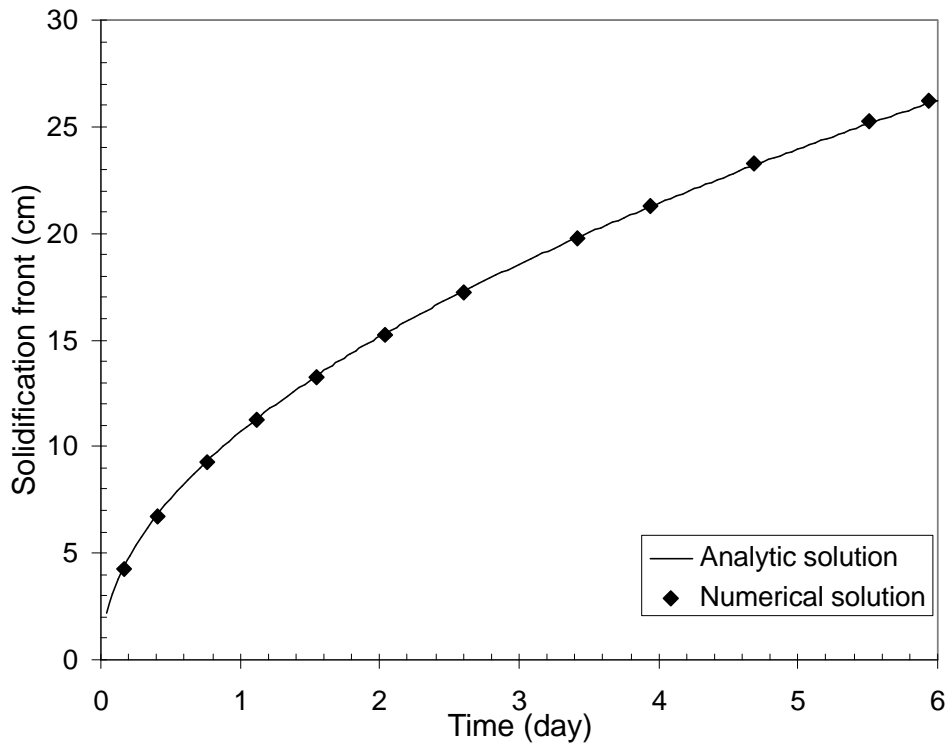


Figure 2. Position of the phase change interface vs. time for the classical Stefan problem

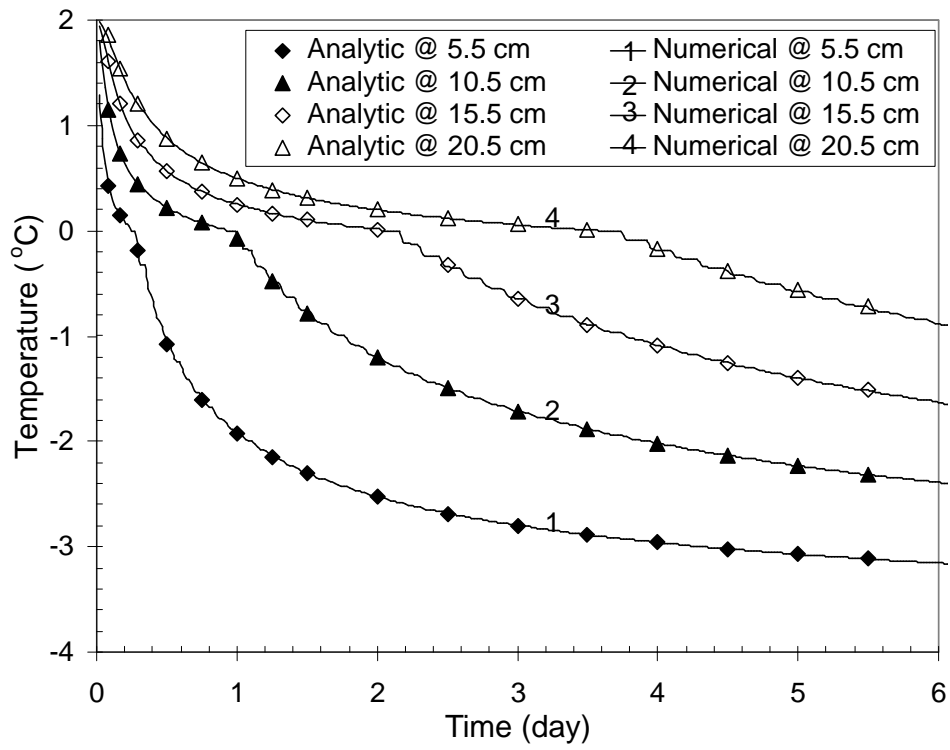


Figure 3. Comparison of numerical and analytic temperature history at several positions for the classical Stefan problem

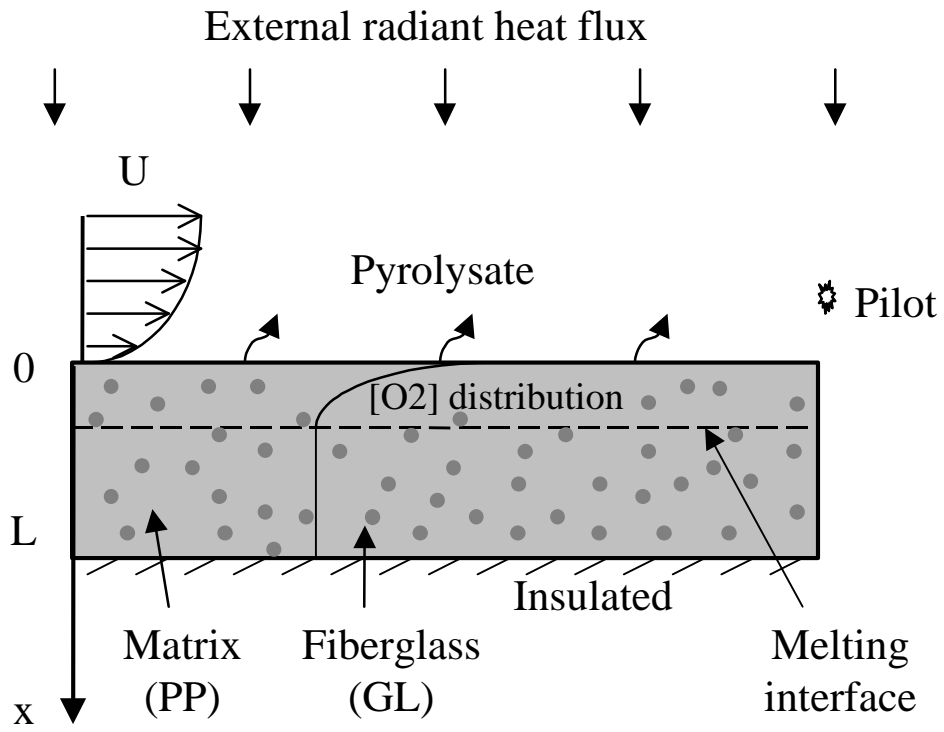


Figure 4. Schematic of the pyrolysis and ignition of a composite

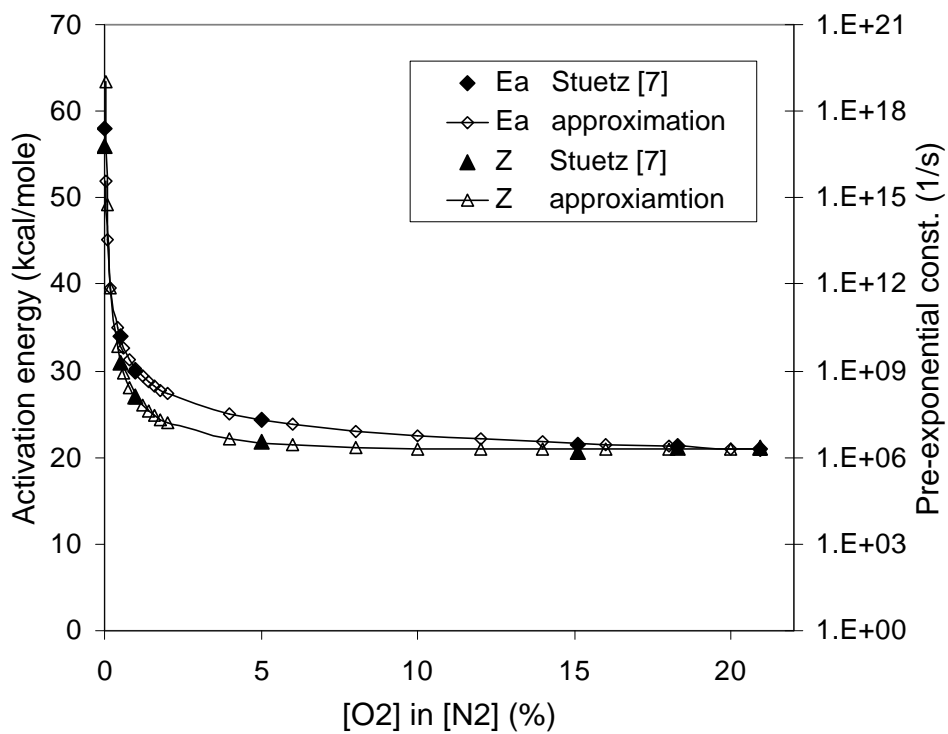


Figure 5. Pre-exponential constant and activation energy as a function of oxygen concentration

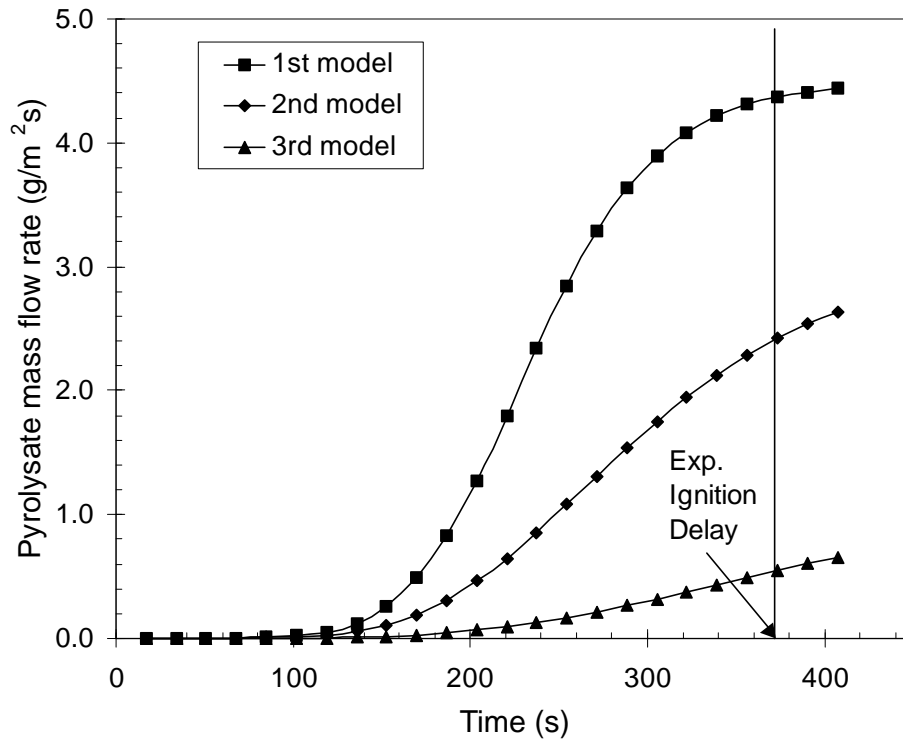


Figure 6. Predicted oxygen concentration effect on the pyrolysate mass flow rate for the three models of oxygen distribution

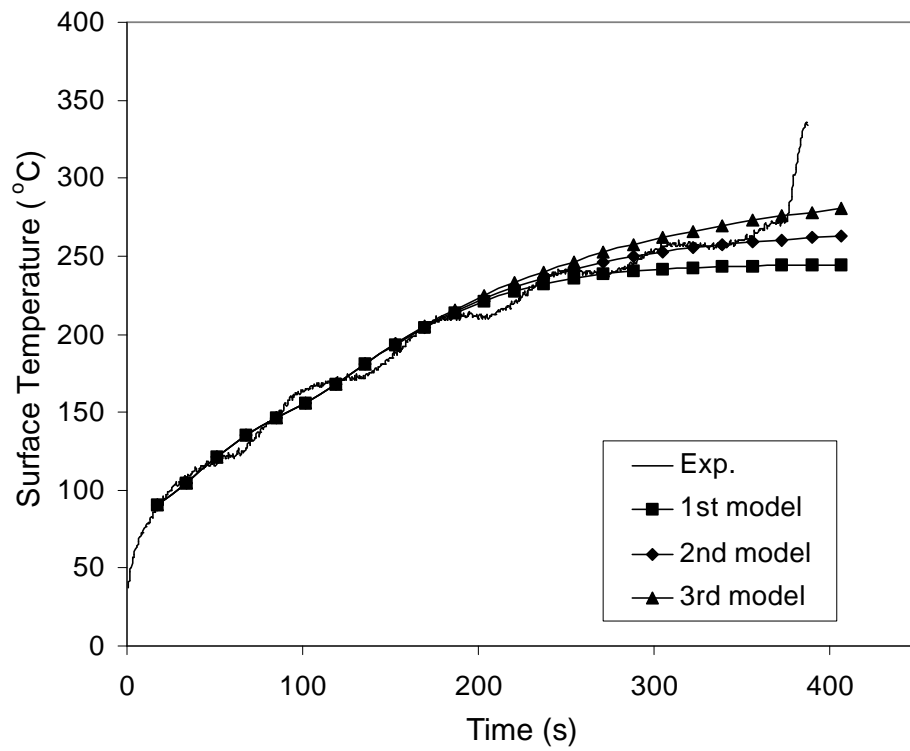


Figure 7. Predicted variation with time of the sample surface temperature for the three models

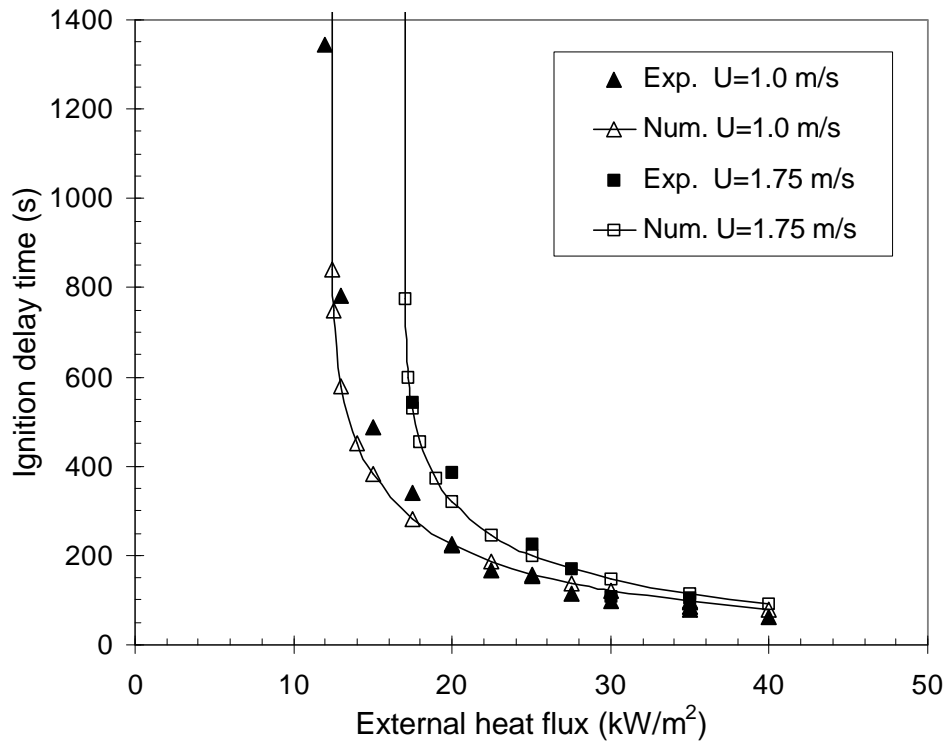


Figure 8. Predicted external heat flux effect on ignition delay for two flow velocities using the second model